Biochimica et Biophysica Acta, 597 (1980) 587—602

BBA 78658

POTENTIAL-DEPENDENT INTERACTION OF TOXIN FROM VENOM OF THE SCORPION *BUTHUS EUPEUS* WITH SODIUM CHANNELS IN MYELINATED FIBRE

VOLTAGE CLAMP EXPERIMENTS

G.N. MOZHAYEVA [a], A.P. NAUMOV [a], E.D. NOSYREVA [a] and E.V. GRISHIN [b]

[a] *Institute of Cytology, Academy of Sciences of the U.S.S.R., Leningrad 190121 and* [b] *Institute of Bioorganic Chemistry, Academy of Sciences of the U.S.S.R., Moscow 117312 (U.S.S.R.)*

(Received May 1st, 1979)
(Revised manuscript received September 3rd, 1979)

Key words: Voltage clamp; Na^+ channel; Scorpion toxin; Binding constant; (Nodal membrane)

Summary

1. The steady-state characteristics of the sodium channel gating in the nodal membrane were determined under voltage clamp conditions before and after treatment with toxins from the venom of scorpion, *Buthus eupeus*.

2. The apparent binding constant (K_A) of the toxin was determined for different levels of the membrane potential. At potentials more negative than −120 mV, K_A tends to a constant level. K_A is maximum at about −80 mV, and it decreases as the potential is reduced to 0 mV.

3. A model assuming that the voltage dependency of K_A is mainly due to the difference in electrical energy between inactivated states of normal and poisoned channels is proposed. An additional decrease in overall binding of toxin results from the transition of a fraction of the sodium channels into the state of slow inactivation.

Koppenhöfer and Schmidt [1] reported that the venom from the scorpion, *Leiurus quinquestriatus*, slows down the inactivation process of sodium channels in the nodal membrane. A similar effect has been demonstrated in the squid giant axon working with the venom from the scorpion, *Buthus tamulus* [2]. Subsequent studies showed that the specific effect of scorpion venoms must be attributed to some of their polypeptide components, the so-called scorpion toxins [3—5]. The effect is produced at very low concentrations

(10^{-7}—10^{-9} M), which suggests the existence of specific receptors.

Catteral et al. [6,7] have shown that the binding of toxin from *L. quinquestriatus* venom to receptors in the neuroblastoma membrane (presumably sodium channels) is considerably reduced by increasing the potassium concentration in the external medium. A decrease in the binding of some of the toxins from the scorpion, *B. eupeus*, induced by depolarization of the nodal membrane has been demonstrated in the study of Mozhayeva et al. [8]. The data lent support to the idea that the observed decrease in the binding of the toxins induced by depolarization is due to a potential-dependent transition of the sodium channel, from a high to low affinity state. To understand the cause of voltage dependency of the toxin binding it seems necessary to determine, firstly, the binding constant of the toxin-channel complex at different levels of the membrane potential, and secondly, the steady-state parameters of such potential dependency such as fast inactivation, slow inactivation and peak sodium conductance both for normal and toxin-poisoned sodium channels.

Toxins (hereafter referred to as M_7 and 2001) from the venom of scorpion, *B. eupeus*, were used in our investigation. These toxins are basic polypeptides with molecular weights in the range 6000—8000. The procedure of purification and their biochemical properties have been described before [9].

Materials and Methods

The work was done on myelinated nerve fibres from the frog, *Rana ridibunda*, using a voltage clamp technique described before [10]. Leakage and slow capacitative currents were subtracted automatically with an analogue electronic device. To estimate the membrane current (I_{Na}), the resistance of the current-feeding internode was assumed to be equal to 15 MΩ. Membrane voltage (V_M) was referred to the outside. I_{Na} was measured in response to the test pulse (V_T) which was preceded by a prepulse (V_C) of 100 ms duration. Holding potential (V_H) is V_M between current measurements.

External solutions contained: (1), 110 mM Na^+, 2 mM Ca^{2+}, 5 mM $Tris^+$, 10 mM tetraethylammonium$^+$ and 120 mM Cl^-; (2), 30 mM Na^+, 80 mM choline$^+$, 5 mM $Tris^+$, 10 mM tetraethylammonium$^+$, 2 mM Ca^{2+} and 129 mM Cl^-, pH 7.3—7.4. Tetraethylammonium ions were added to block current through potassium channels [11—13]. Scorpion toxins were added to solutions 1 and 2. The ends of the fibres were cut in a solution containing 120 mM KF.

Voltage current relations and chord conductances (g_p) can be adequately measured only if the series resistance (R_S) is small, or if compensated feedback amplifiers are used [14—16]. To measure the distortion in g_p-curves due to R_S, inward I_{Na} was reduced either by reducing the conditioning potential level from —140 to —80 mV, or by using choline$^+$ in place of Na^+ (compare solutions 1 and 2). After toxin treatment only the second method was used. The absence of changes in steepness and position of g_p-curves after reduction of sodium current was taken to indicate that effects of R_S may be neglected. The experiments were carried out at 8—10°C.

Results

Fig. 1 shows records of the currents before (a) and after (b, c, d) application of toxin M_7 at three concentrations (C_T). The development of the toxin effect

took several minutes at C_T values higher than $1 \cdot 10^{-6}$ M and, 20—25 min at C_T values lower than $1 \cdot 10^{-7}$ M. It can be seen in Fig. 1 that the rate of the I_{Na} inactivation is decreased and steady-state I_{Na} appears. It is also apparent that the higher the C_T, the greater the steady-state level of I_{Na} (at any particular potential). For a C_T value higher than $1 \cdot 10^{-6}$ M, this steady-state level of I_{Na} did not increase and the reduced rate of inactivation remained unaffected. The treatment of the membrane with scorpion toxins results, as a rule, in some reduction of the sodium currents. This effect seems to be nonspecific since it varies considerably for different fibres. The effects of toxin 2001 are very similar, although it is more potent than toxin M_7.

An analysis of the kinetic parameters of the sodium currents in normal and poisoned nerve fibres will be given elsewhere. In the present work, we compared the steady-state parameters of the potential-dependent characteristics of both normal and poisoned channels with the potential-induced changes in the binding of toxin to the channel. Comparing data from different fibres increases the error due to intrinsic variations between different fibres and gradual deterioration of the axons during long-lasting runs between 1.5 and 2 h. In order to minimize these effects, the measurements were repeated before and

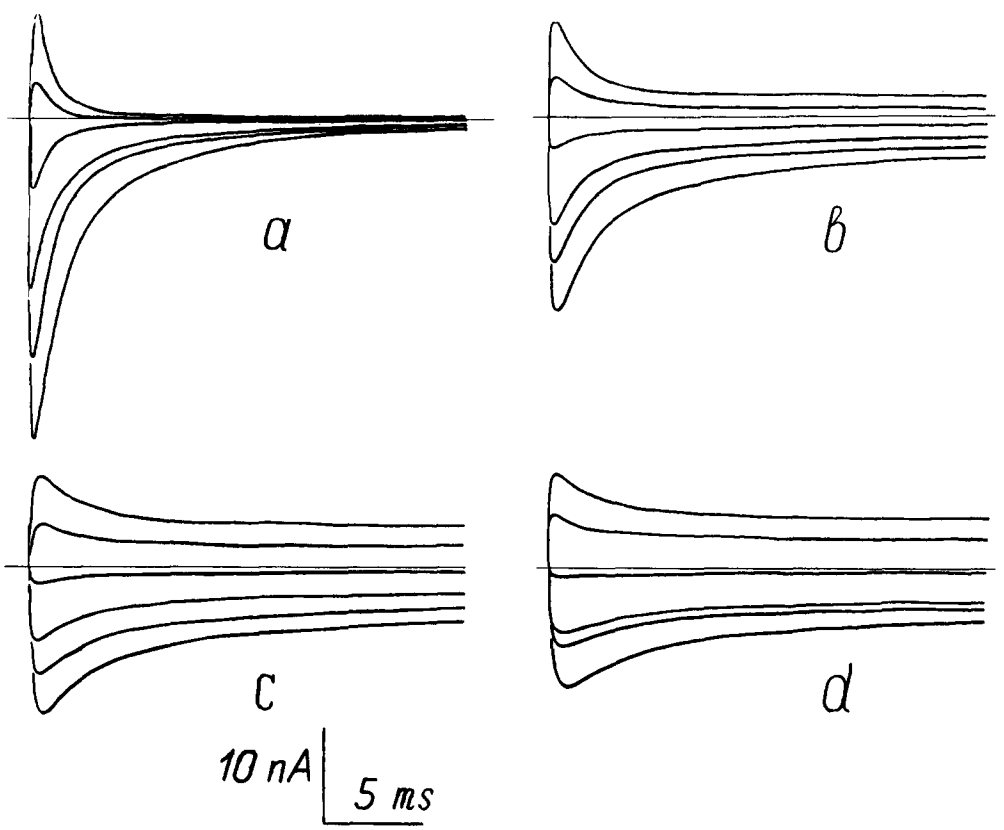

Fig. 1. Sodium currents before (a) and after successive applications of toxin M_7 at three concentrations; (b) 13 min, $1 \cdot 10^{-7}$ M; (c) 10 min, $3.3 \cdot 10^{-7}$ M; and (d) 8 min, $1 \cdot 10^{-6}$ M. $V_H = -100$ mV, $V_C = -140$ mV (100 ms); potentials during test pulses are —10, +10, +20, +40, +60 and +80 mV; Node 146.

TABLE I

PARAMETERS OF DEPENDENCE OF PEAK CONDUCTANCE (SUBSCRIPTS g AND 2) AND OF STEADY-STATE FAST INACTIVATION (SUBSCRIPTS h AND 3) ON POTENTIAL DETERMINED IN ACCORD WITH EQNS. 11 AND 12

Node	Control				Toxin			
	$a_g = a_2$ (mV^{-1})	$V_g = V_2$ (mV)	$a_h = a_3$ (mV^{-1})	$V_h = V_3$ (mV)	$a_g^* = a_2^*$ (mV^{-1})	$V_g^* = V_2^*$ (mV)	$a_h^* = a_3^*$ (mV^{-1})	$V_h^* = V_3^*$ (mV)
114			0.129	−88.1			0.103	−86.1
179	0.110	−34.3			0.090	−37.1		
185	0.102	−26.6			0.130	−28.9		
223	0.140	−29.0	0.127	−77.6			0.086	−76.5
224			0.123	−78.6			0.097	−82.8
226			0.166	−68.0	0.150	−35.0	0.102	−70.9
228	0.130	−34.0	0.141	−69.9	0.130	−41.0	0.083	−71.4
239	0.110	−17.5	0.106	−93.5	0.120	−18.3	0.079	−89.6
240			0.154	−74.4			0.080	−91.9
242			0.163	−73.2			0.105	−80.6
246	0.120	−27.3					0.090	−75.4
249	0.145	−38.0	0.178	−88.3	0.145	−42.0	0.080	−84.9
260			0.129	−82.5			0.095	−107.3
262			0.102	−82.0			0.075	−86.0
264	0.130	−27.8	0.130	−87.3	0.130	−37.7	0.087	−78.6
265	0.122	−22.0			0.120	−20.0		
266	0.160	−35.0	0.120	−78.7	0.130	−36.7	0.110	−77.2
267	0.114	−27.4	0.121	−72.0	0.114	−30.2	0.078	−72.0
268	0.161	−23.2	0.151	−70.6	0.151	−25.1	0.081	−76.8
269	0.132	−31.9			0.113	−32.9		
Mean	0.129	−28.8	0.136	−79.0	0.127	−32.0	0.089	−81.7
± S.D.	± 0.018	± 5.8	± 0.021	± 7.8	± 0.017	± 7.7	± 0.011	± 9.4

after treatment with toxin on the same fibre. Steady-state voltage-dependent parameters of the fast inactivation and the peak conductance for normal and treated fibres are summarized in Table I.

Steady-state inactivation

Steady-state inactivation curves ($h_\infty - V_M$) were determined using conventional double-pulse protocols. The test pulse (0.3—0.4 ms in duration), to +80 mV, was kept constant while the prepulse, 100 ms in duration, varied from the holding potentials towards hyperpolarized and depolarized levels. Fig. 2 shows the fraction of the sodium channels available to conduct I_{Na} at the end of the prepulse (h_∞) as a function of potential before and after application of $1 \cdot 10^{-6}$ M toxin M_7. It may be seen that the h_∞-curve for the treated axon is less steep than that for the control fibre. In order to evaluate the effects on $h_\infty - V_M$ we used the empirical equation:

$$h_\infty = \frac{1}{1 + \exp a_h(V_M - V_h)} \tag{1}$$

where a_h = steepness factor (in mV^{-1}), V_h = potential of half inactivation. Eqn. 1 describes h_∞-curves both for normal and poisoned channels rather well at potentials more negative than −50 mV. Therefore, the fitting of the points

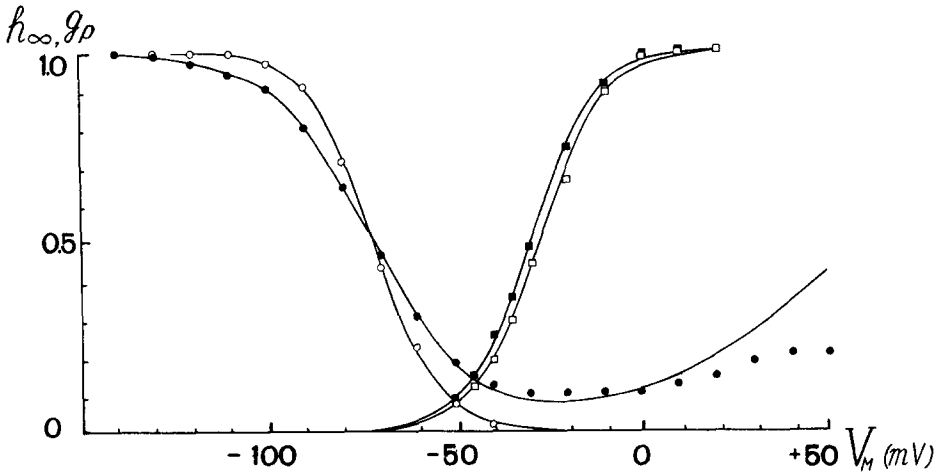

Fig. 2. The dependence of fast steady-state inactivation (h_∞) (circles) and normalized peak sodium conductances (g_p) (squares) on membrane potential before (○ and □) and after (● and ■) treatment with $1 \cdot 10^{-6}$ M toxin M_7. Solid lines are calculated from Eqns. 11, (h_∞-curves) and 12 (g_p-curve) with the following parameter values: $a_3 = 0.121$ mV^{-1}, $V_3 = -72.0$ mV; $a_2 = 0.114$ mV^{-1}, $V_2 = -27.4$ mV for normal channels; and $a_3^* = 0.078$ mV^{-1}, $V_3^* = -72.0$ mV, $a_2^* = 0.114$ mV^{-1}, $V_2^* = -30.2$ mV for poisoned channels. $V_H = -100$ mV; Node 267.

with Eqn. 1 was confined over this potential range. Parameters a_h and V_h were evaluated for each experiment by the least-square method.

In the experiment presented in Fig. 2, $a_h = 0.121$ and 0.078 mV^{-1} for normal and treated fibres, respectively. The decrease in a_h was invariably reproduced in all experiments. Individual and averaged a_h values are also presented in Table I. The average a_h is 0.136 mV^{-1} and $a_h^* = 0.089$ mV^{-1} (the asterisk represents treated axons). It is clear that the toxin does not affect significantly the position of the h_∞-curve on the voltage axis. The average V_h was -79.0 mV for the control runs and -81.7 mV for the treated fibres.

The h_∞-curve for poisoned fibres shows a secondary branch which rises at potentials from -30 to -40 mV and saturates at positive potentials. Saturated h_∞^* values vary considerably (from 0.10 to 0.45).

Toxin 2001 induced similar changes on the h_∞-curve. A similar effect on the steady-state inactivation curve was shown earlier with *Leiurus quinquestriatus* venom [1].

Peak sodium conductance

Fig. 2 shows g_p-curves obtained before and after treatment with $1 \cdot 10^{-6}$ M toxin M_7, normalized to their maximum g_p values. It is seen that treatment with the toxin results in a slight shift of the g_p-curve towards more negative potentials. No change in the slope is seen. The normalized g_p-curve is reasonably well described by the empirical equation:

$$g_p = \frac{\exp a_g(V_M - V_g)}{1 + \exp a_g(V_M - V_g)} \tag{2}$$

where a_g and V_g are the steepness factor and the potential for half conductance, respectively. Individual values of these parameters (calculated by the

least-squares method) for each experiment are presented in Table I. The average values for untreated axons are $a_g = 0.129$ mV^{-1} and $V_g = -28.8$ mV; and for poisoned axons, $a_g^* = 0.127$ mV^{-1} and $V_g^* = -32.0$ mV.

We did not measure the rates of sodium conductance increase at various depolarizations before and after toxin treatment. Experiments where I_{Na} was measured with adequate speed sweep showed that the toxin caused little or no change in the rate of increase of the inward I_{Na}. In the majority of the experiments, however, there was a slowing down of the 'tail' currents during repolarization. In this respect, the effects of scorpion toxin are similar to those of the trinitrophenol [17].

Steady-state slow inactivation

Besides the fast inactivation process (the h-process in the Hodgkin and Huxley terminology), there are several reports on the existence of a rather slow process (time constant is of the order of seconds). It is referred to as a slow inactivation process (S-process) [18—22].

To determine the potential-dependence of the S-process, I_{Na} records, in response to a test pulse to +80 mV, were measured from the different holding-potential levels. To remove fast inactivation, every V_T was preceded by $V_C = -140$ mV, 100 ms in duration. Control experiments showed that variations in prepulse length from 20 to 300 ms do not affect the sodium current values. Hence, it could be concluded that the prepulse removed fast inactivation alone, without affecting the S-process. When studying S-inactivation of poisoned channels, in order to prevent dissociation of the toxin-channel complex during long-lasting depolarization (see below), we used toxin 2001 at a high concentration ($5 \cdot 10^{-6}$ M).

The decay of I_{Na} in response to a depolarizing holding-potential commonly has two stages; a fast stage (10—20 s), and a slow stage (1.5—5 min), depending on V_H. The fast stage accounts for a greater part of the I_{Na} reduction observed. The slow phase seems to be due both to the S-process, and to some irreversible damage of sodium conductance, which is pronounced at low V_H values. In order to minimize the influence of this irreversible damage on the evaluation of the S-process under steady-state conditions, measurements of I_{Na} from low V_H were alternated with measurements from $V_H = -120$ mV. S_∞ values were calculated as follows:

$$S_\infty = \frac{2 \cdot I_{V_H}}{I'_{-120} + I''_{-120}} \tag{3}$$

where $I_{V_H} - I_{Na}$ was measured from a particular V_H level and I'_{-120} and $I''_{-120} - I_{Na}$ from $V_H = -120$ mV before and after depolarization. All values in this formula represent steady-state levels of I_{Na} for each V_H value.

Fig. 3 shows the S_∞-curve for the control and experimental runs. As in the case of nodal membrane from *Rana esculenta* [19], *Xenopus laevis* [21] and axonal membrane from squid [22], S_∞-curves in our case are shifted in the direction of more positive potentials as compared with h_∞-curves. The solid lines in Fig. 3 were calculated using the empirical equation:

$$S_\infty = \frac{1}{1 + \exp a_S(V_M - V_S)} \tag{4}$$

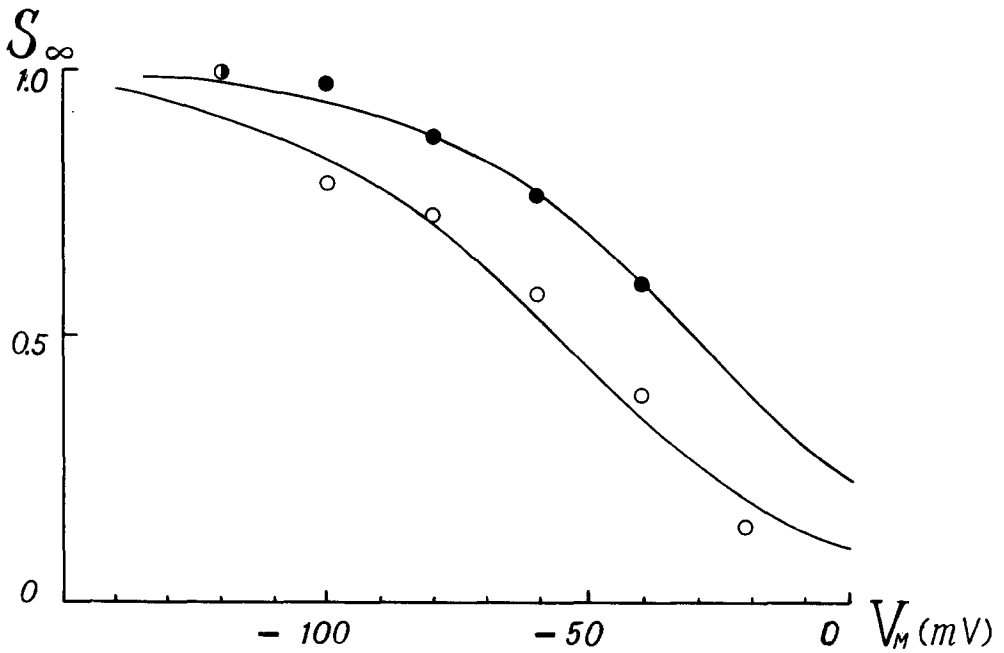

Fig. 3. Voltage-dependence of steady-state slow inactivation before (○) and after (●) application of $5 \cdot 10^{-6}$ M toxin 2001. Solid lines are calculated from Eqn. 4 with the following values of parameters: a_S = 0.039 mV^{-1}, V_S = −57.3 mV for normal channels; and a_S^* = 0.040 mV^{-1}, V_S^* = −30.5 mV for poisoned channels. V_C = −140 mV (100 ms); Node 119.

where a_S and V_S are the steepness factor and potential of half inactivation, respectively. Eqn. 4 was fitted to the points by means of the least-squares method. For the data presented in Fig. 3, we have a_S = 0.039 mV^{-1}, V_S = −57.3 mV, a_S^* = 0.040 mV^{-1} and V_S^* = −30.5 mV. The averages from five experiments (±S.D.) are a_S = 0.046 ± 0.007 mV^{-1}, V_S = −44.1 ± 11.6 mV, a_S^* = 0.044 ± 0.006 mV^{-1} and V_S^* = −21.0 ± 12.5 mV. Thus, scorpion toxin shifts the $S_\infty - V_M$ curves to the right.

Determination of the apparent binding constant (K_A) of the toxin-channel complex

To estimate the fraction of occupied sites, we used differences in inactivation kinetics between normal and poisoned channels. A similar approach has been used before for the analysis of the binding of a toxin from sea anemones [23] and a toxin from *L. quinquestriatus* venom [5].

The test pulse (20—22 ms in duration) took the membrane potential from its holding level to positive potentials (+80 mV). The sodium inactivation could be described using a single exponential. When the test pulse takes the membrane potential to negative values, the records show an inactivation which requires at least two exponential components to be fitted (also see Chiu, Ref. 24). To minimize the dissociation of the toxin-channel complex during the pulse, the duration of the test pulse was limited to 20—22 ms. That such dissociation exists has been shown before in experiments with long-lasting pulses [8].

Fig. 4 presents semi-logarithmic graphs of the sodium currents at V_T = +80

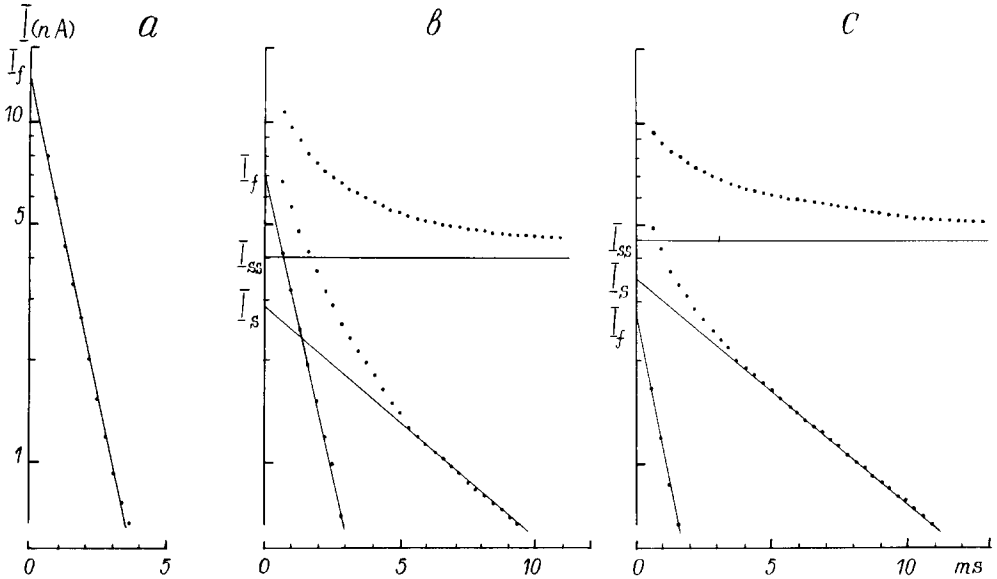

Fig. 4. Semi-logarithmic plot of sodium currents before (a) and after application of toxin M_7; (b) 10 min, $3.3 \cdot 10^{-7}$ M; (c) 8 min $1 \cdot 10^{-6}$ M. $V_H = -100$ mV, $V_C = -140$ mV (100 ms), $V_T = +80$ mV (See text for details); Node 146.

mV before and after application of toxin M_7 at concentrations of $3.3 \cdot 10^{-7}$ and $1 \cdot 10^{-6}$ M. It is seen that before toxin application, the decay of current can be described by the single exponent with a time constant (τ_f) equal to 1.2 ms. In the presence of toxin, the total current can be separated into at least three components: (1) a fast component, with a time constant equal to that before toxin treatment (τ_f); (2) a slow component, with a time constant (τ_S) equal, in this experiment, to 6.6 ms; (3) a steady-state level, with a time constant too large to measure. It can be seen that the slow and steady-state components increase when toxin concentrations are increased. We suggest that the slow and steady-state components represent sodium current through the modified sodium channels, and that the fast component represents sodium current through the normal channels. The fraction (θ) of the poisoned channels may be expressed by the equation:

$$\theta = \frac{I_{SS} + I_S}{I_{SS} + I_S + I_f} \tag{5}$$

where I_{SS}, I_S and I_f are extrapolated values of steady-state, slow and fast components at zero time. Assuming a unimolecular reaction between the toxin molecule and the channel, the equilibrium binding constant (K_A) will be given by the equation:

$$K_A = \frac{\theta}{C_T(1-\theta)} \tag{6}$$

This assumption is based on the observation that the K_A values calculated using Eqn. 6 are practically independent of the concentration used in the experiment. Thus, K_A values calculated from results of the experiment in Fig. 4 at

$V_H = -100$ mV turned out to be almost equal at $0.33 \cdot 10^7$, $0.31 \cdot 10^7$ and $0.30 \cdot 10^7$ M^{-1} for C_T values $1 \cdot 10^{-7}$, $3.3 \cdot 10^{-7}$ and $1 \cdot 10^{-6}$ M, respectively. On the average from 13 experiments, K_A for toxin M_7 at $V_H = -100$ mV is equal to (±S.D.) $(0.93 \pm 0.58) \cdot 10^7$ M^{-1}. Toxin 2001 appears to be bound to the receptor more tightly than M_7. The average value (from five experiments) at $V_H = -100$ mV is equal to (±S.D.) $(2.6 \pm 0.4) \cdot 10^7$ M^{-1}.

Dependence of K_A on membrane potential

To determine the effects of potential on K_A, the steady-state values of the fraction of the affected channel at different V_H levels were measured. Fig. 5 shows the results of one of the experiments. Toxin M_7, at a concentration of $3 \cdot 10^{-7}$ or $1 \cdot 10^{-7}$ M, was added to the external solution while the membrane potential was held at −100 mV. I_{Na} in response to a +80 mV pulse was measured at intervals of 10—20 s. Test pulses were preceded by a conditioning prepulse $V_C = -140$ mV, 100 ms in duration. This prepulse was sufficient to remove fast inactivation but too short to change θ. It has been further assumed that when I_{Na} stopped changing, θ attained a steady-state level (in the experiment presented here it took about 25 min). Measurements of θ were repeated several times. Thus, in one experiment (a part of which is presented in Fig. 5)

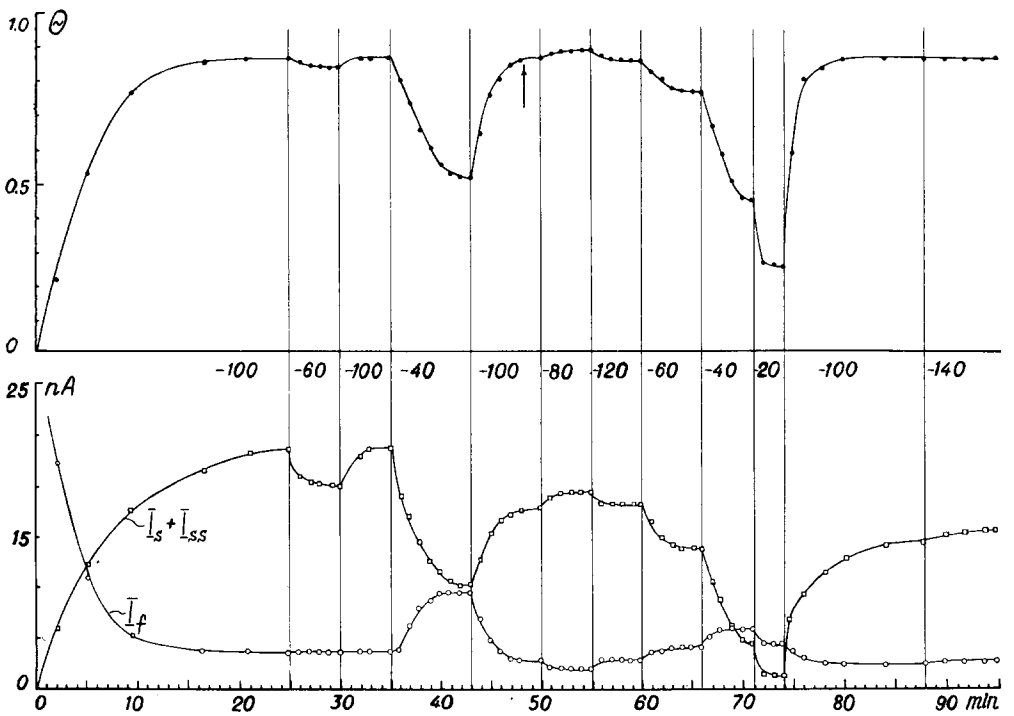

Fig. 5. Effect of holding potential on toxin M_7 binding with the sodium channels. The upper half depicts the fraction of the poisoned channels, θ, (●). The lower half depicts the amplitudes of currents through normal (○) and through poisoned channels (□). The numbers in the middle are the holding potentials. $V_T = +80$ mV, $V_C = -140$ mV (100 ms). The arrow points to the time when h^*_∞ and g^*_p curves presented in Fig. 6 were measured; Node 226.

determinations of θ at $V_H = -100$ mV were carried out four times, and at $V_H = -120$, -140, -60 and -40 mV, twice.

It should be noted that 100 ms prepulses to negative potentials cannot remove the slow inactivation which develops during long-lasting depolarizations. That is why θ values and corresponding K_A values obtained in the above experiments measure properties of unaffected channels.

Shown in Fig. 5 are values of currents both through poisoned ($I_{SS} + I_S$) and normal (I_f) channels, and θ values at different V_H levels. It may be seen that depolarization of the membrane below -80 mV results in a decrease of θ, which at V_H -60 and -40 mV is due to a decrease in absolute values of the slow and steady-state components and an increase in the fast component. In a number of experiments, the increase in the absolute value of the fast component of the I_{Na} was observed, even at $V_H = -20$ mV. These observations indicate that upon depolarization, a part of the toxin-channel complex, formed at high negative potentials, is dissociated.

Further, it can be seen in Fig. 5 that changing V_H from -100 to -80 mV results in a small, but quite clear increase in θ, and an increase from -80 to -120 mV results in a decrease of θ. Table II presents K_A values at different holding potentials for nine experiments. K_A values for each experiment were normalized to those values at $V_H = -140$ mV. When the determinations of θ were repeated, K_A was calculated using an average θ value. Normalized K_A values for the experiment presented in Fig. 5 are plotted in Fig. 6 as a function of potential. In the same figure, h_∞-curves obtained before and after toxin application are shown. At $V_H = -100$ mV, $\theta = 0.86$; thus, the inactivation curve obtained in this case can be regarded as that representing poisoned channels. The following features of the potential-dependency of K_A are noteworthy: (1) K_A reaches a constant level at very negative membrane potentials (-120 to -140 mV); (2) K_A has a maximum at $V_H = -80$ mV. In

TABLE II

APPARENT BINDING CONSTANT (K_A) FOR TOXIN M_7 AT DIFFERENT LEVELS OF MEMBRANE POTENTIAL

K_A values are normalized to those at $V_H = -140$ mV. The numbers in parentheses denote the number of determinations of the fraction of the poisoned channels (θ) when it was more than 1. In this case, K_A was calculated using the mean θ value.

Node	K_A						
	Membrane potential (mV)						
	−120	−100	−80	−60	−40	−20	0
98		1.23	0.97	0.47			
99		1.18	1.30	0.52			
100	1.11	1.08	0.97	0.56			
114	1.06 (2)		1.35	0.52		0.03	
215	1.08 (2)	1.14 (2)		0.53			0.03
223	1.08	1.10 (2)		0.58	0.26		0.04
226	1.00 (2)	1.07 (4)	1.26	0.75 (2)	0.16 (2)	0.05	0.05
228	1.04 (2)	1.18 (4)	1.31	0.59	0.21	0.09	
242	1.02	1.04 (2)	1.18	0.69	0.21	0.11	0.05
Mean ± S.D.	1.06 ± 0.04	1.13 ± 0.07	1.19 ± 0.16	0.58 ± 0.09	0.21 ± 0.04	0.07 ± 0.04	0.04 ± 0.01

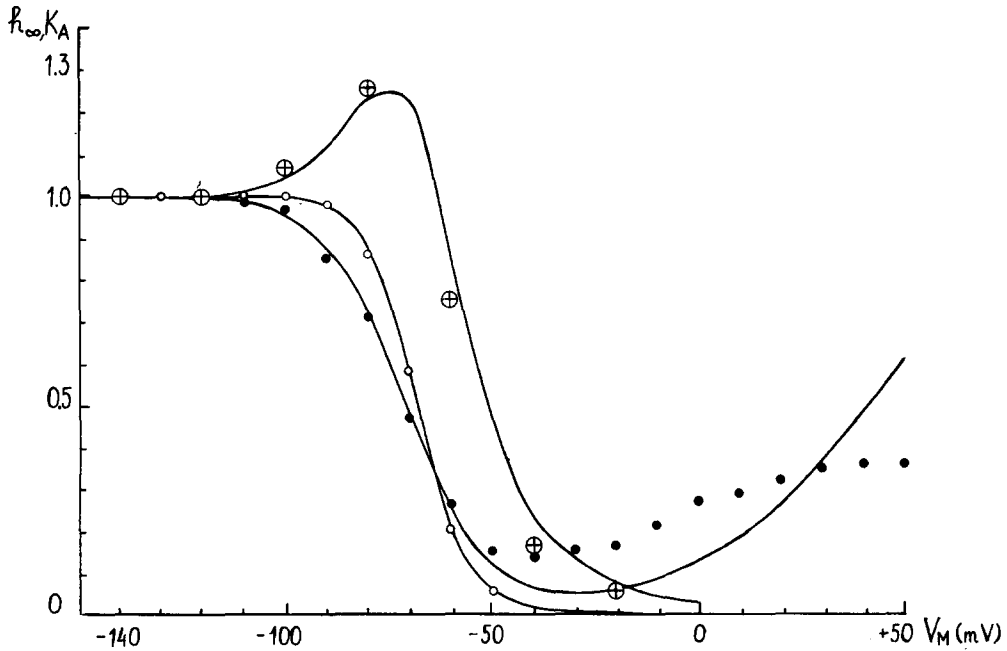

Fig. 6. Potential-dependence of the normalized binding constant of toxin M_7 (⊕) and steady-state sodium inactivation of normal (○) and poisoned (●) channels. Solid lines are calculated from Eqns. 14 (K_A curve) and 12 (h_∞ curves) with the following values of parameters: $a_2 = a_2^* = 0.150$ mV^{-1}, $V_2 = V_2^* = -35.0$ mV, $a_3 = 0.166$ mV^{-1}, $V_3 = -68.0$ mV, $a_3^* = 0.102$ mV^{-1}, $V_3^* = -70.9$ mV. See text for details; Node 226.

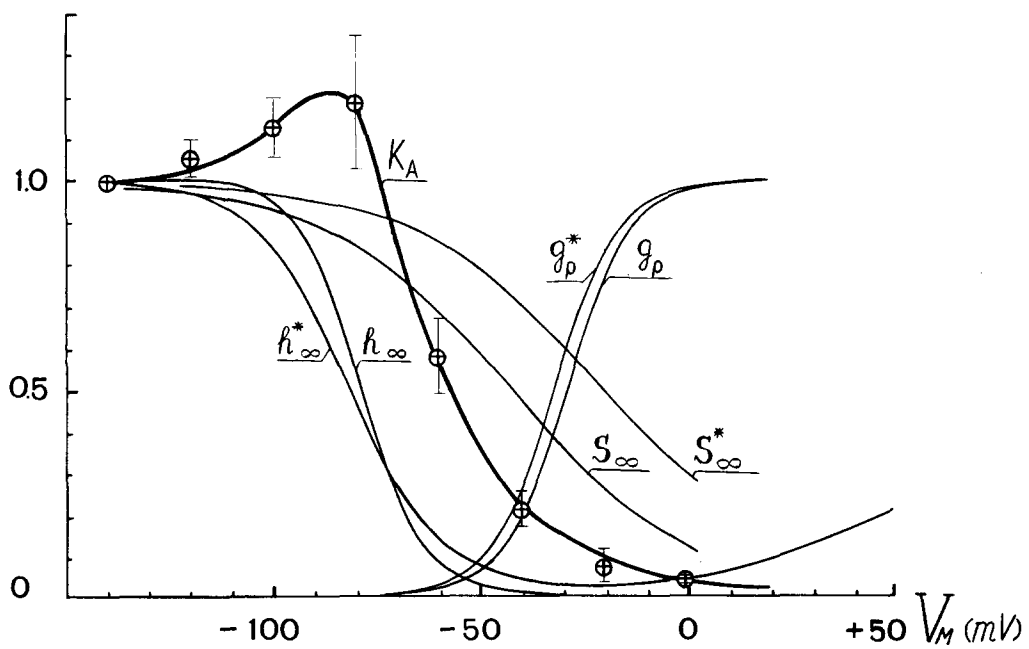

Fig. 7. Apparent binding constant (K_A) of toxin, steady-state fast inactivation (h_∞ and h_∞^*), peak conductance (g_p and g_p^*) and steady-state slow inactivation (S_∞ and S_∞^*) as functions of the membrane potential. Asterisks denote curves relevant to the channels poisoned by toxin. Circles represent mean K_A values from Table II, vertical bars depict ±S.D. Solid lines are calculated from Eqns. 4, 11, 12 and 14 with mean values of parameters (see Table I and text).

the majority of the experiments (see Table II), the maximum K_A value occurs at −80 or −100 mV; (3) K_A decreases as V_M becomes less negative; (4) the declining part of the K_A-V_M curve is shifted to the right relative to the h_∞-curve.

Average normalized K_A values are presented in Table II and plotted in Fig. 7 as a function of potential. K_A attains its maximum value at $V_H = -80$ mV. A shift of V_H from −80 to 0 mV results in a 28-fold reduction of K_A, and a shift of V_H from −80 to −140 mV results in a 1.2-fold reduction of K_A.

Analysis and Discussion

The toxins used in the present work are positively charged at normal pH values. Therefore, the electric field may act directly on the toxin molecules, thus altering the apparent equilibrium binding constant. On theoretical grounds, K_A should change exponentially with respect to potential. However, the experiment showed that K_A changed exponentially only at potentials less negative than −60 mV. At more negative potentials, K_A tends to a constant level. Thus, this assumption is not supported by experimental data.

The idea that gating processes are due to conformational changes of gating structures in the membrane has become widely accepted [25]. Since depolarization of the membrane favours the opening and inactivation of the sodium channels, it is natural to assume that the decrease in K_A with depolarization is due to a channel transition from a closed, non-inactivated state, with a high K_A value, to an open or inactivated state, with a low K_A value. To examine the possibility of such an explanation we shall consider the following model.

Let us assume that the sodium channel has two gate mechanisms, m- and h-mechanisms, following the Hodgkin-Huxley model notations [26]. Let us further assume two possible states for each of them: closed and open, non-inactivated and inactivated. Then, a sodium channel, as a whole, can assume four states: (1) closed non-inactivated; (2) open non-inactivated; (3) closed inactivated; (4) open inactivated. So there are two inactivated states, 3 and 4, and only one conducting state, 2. All these states differ in that they have different potential-dependent free energy levels. If we consider the free energy level of the first state as a reference, and denote the free energies of the remaining states as ΔG_2, ΔG_3 and ΔG_4, respectively, the free energy of any state may be represented as a sum of two components: potential-dependent and potential-independent components. Let us assume that the free energy is a linear function of potential. Then, free energy (in kT units) of the channel in state i will be given by the equation:

$$\Delta G_i = -a_i V_M + \Delta G_{oi} = -a_i(V_M - V_i) \tag{7}$$

where ΔG_{oi} is the potential-independent component of free energy; $V_i = \Delta G_{oi}/a_i$, the potential (in mV) at which $\Delta C_i = 0$; a_i = steepness factor, in mV^{-1} (describing the sensitivity of a particular transition to the electric field). Another widely-used measure of this sensitivity is a so-called effective charge $z_{efi} = a_i kT/e$.

Let us denote equilibrium fractions of the channels in states 1, 2, 3 and 4 or probabilities of channels being in these states as n_1, n_2, n_3 and n_4. According

to the usual thermodynamics and condition of normalization we obtain a set of equations:

$$\begin{aligned} n_2/n_1 &= \exp - \Delta G_2 \\ n_3/n_1 &= \exp - \Delta G_3 \\ n_4/n_1 &= \exp - \Delta G_4 \\ n_1 + n_2 + n_3 + n_4 &= 1 \end{aligned} \tag{8}$$

Substitution of the expression for free energy (Eqn. 7) in the set of equations (Eqn. 8) gives expressions for the fraction of non-inactivated channels (h_∞) and the steady-state normalized conductance (g_∞) as follows:

$$h_\infty = n_1 + n_2 = \frac{1 + \exp a_2(V_M - V_2)}{1 + \exp a_2(V_M - V_2) + \exp a_3(V_M - V_3) + \exp a_4(V_M - V_4)} \tag{9}$$

$$g_\infty = n_2 = \frac{\exp a_2(V_M - V_2)}{1 + \exp a_2(V_M - V_2) + \exp a_3(V_M - V_3) + \exp a_4(V_M - V_4)} \tag{10}$$

The use of Eqn. 9 hinges on another problem; whether m and h are interdependent processes. If they are independent of each other, then parameters for the m-transition, from closed to open states, should be independent of the state of the h-gate, i.e., parameters of the 3—4 transition should be equal to parameters of the 1—2 transition. Hence, for $a_2 + a_3 = a_4$, Eqn. 9 predicts that h_∞ should tend to zero at positive potentials. This prediction is not supported by the data; there is a rising of the h_∞-V curve at positive potentials. Besides, a non-zero level of h_∞ at positive potentials is observed in squid axon even under normal conditions [27]. Thus, we have to assume that the m- and h-mechanisms are coupled. Let us assume that the development of inactivation immobilizes the gate completely. Then, Eqn. 9 can be simplified to:

$$h_\infty \simeq \frac{1 + \exp a_2(V_M - V_2)}{1 + \exp a_2(V_M - V_2) + \exp a_3(V_M - V_3)} \tag{11}$$

Comparing Eqn. 11 with Eqn. 1 shows that if Eqn. 1 is interpreted as describing a distribution between closed non-inactivated and inactivated states only, then the parameters a_3 and V_3 from Eqn. 11 may be equated to parameters a_h and V_h from empirical Eqn. 1.

Experiments on internally-perfused giant axons showed that the potential-dependency of the steady-state conductance, after removing inactivation by pronase [28], is similar to that of the peak conductance before treatment with pronase. Thus, peak conductance may be regarded as a measure of the equilibrium distribution of channels between states 1 and 2. Neglecting in Eqn. 10 the terms relevant to the inactivated state, we obtain an equation for the peak conductance as follows:

$$g_p = \frac{\exp a_2(V_M - V_2)}{1 + \exp a_2(V_M - V_2)} \tag{12}$$

This equation is similar to the empirical Eqn. 2. Thus, we can equate parameters a_2 and V_2 to a_g and V_g, respectively.

As seen from Table I, the main difference between treated and untreated

fibres (in terms of the model) is the effective charge for the transition from a non-inactivated to an inactivated state. On average, for the normal channels, $z_{efh} = 3.32$, and for the poisoned channels, 2.17 electronic charges. Accordint to the model, the secondary branch of the h_∞-curve can be explained as follows. In normal channels, free energies of inactivated and open states change in parallel with potential ($a_2 = a_g = a_3 = a_h$, see Eqn. 7). Because V_2 is different to V_3, the energy of the open state is much higher than that of the inactivated state at all potentials. Accordingly, the probability for the open state is much lower. That is why h_∞ values for normal channels at positive potentials are low. For the poisoned channels, $a_h^* = a_3^* < a_2^* = a_g^*$, and therefore, the free energies of open and inactivated states become closer to one another as the membrane potential becomes more positive.

The model does not take into account the possibility that free energies of the channel may be nonlinear functions of potential [29,30] and that the number of the states which the channel can assume is obviously more than three [24,26,28,31]. Nevertheless, the three state model seems to reflect essential traits of distribution of the channels among the most important states. Therefore, we used it to evaluate how transitions of the channel from one state to another affect the toxin binding. The fractions of the channels in possible states as functions of potential and C_T are described by the following set of equations:

$$n_2/n_1 = \exp a_2(V_M - V_2)$$

$$n_3/n_1 = \exp a_3(V_M - V_3)$$

$$n_2^*/n_1^* = \exp a_2^*(V_M - V_2^*)$$

$$n_3^*/n_1^* = \exp a_3^*(V_M - V_3^*)$$

$$n_1 + n_2 + n_3 + n_1^* + n_2^* + n_3^* = 1$$

$$K_1 = \frac{1}{C_T} \cdot \frac{n_1^*}{n_1} \tag{13}$$

where K_1 is the binding constant of toxin for closed non-inactivated channels.

Hence, the apparent binding constant, K_A, is given by:

$$K_A = \frac{1}{C_T} \cdot \frac{n_1^* + n_2^* + n_3^*}{n_1 + n_2 + n_3} = K_1 \cdot \frac{1 + \exp a_2^*(V_M - V_2^*) + \exp a_3^*(V_M - V_3^*)}{1 + \exp a_2(V_M - V_2) + \exp a_3(V_M - V_3)} \tag{14}$$

It is observed that at high negative potentials, K_A tends to K_1. On the other hand, the experiment shows that K_A at high negative potentials tends to a constant level. Thus, it may be concluded that the binding constant of closed non-inactivated channels does not change with potential.

The binding constant of inactivated channels is given by the equation:

$$K_3 = \frac{1}{C_T} \cdot \frac{n_3^*}{n_3} = K_1 \cdot \exp[a_3^*(V_M - V_3^*) - a_3(V_M - V_3)] \tag{15}$$

Since $a_3 > a_3^*$, there is a difference in electrical energy between the inactivated states of normal and poisoned channels. Therefore, the binding constant of an inactivated channel is not constant in fact, and depends on the membrane

potential. At potentials more positive than V_3 and V_3^* it is less than K_1, and at more negative potentials it is greater than K_1.

The calculation similar to the previous one shows that the binding constant for open channels (K_2) does not depend on potential because $a_2 = a_2^*$. On average, K_2 is equal to about 1.5 K_1.

Solid lines in Fig. 6 and 7 represent K_A calculated from Eqn. 14 as a function of potential. The curve in Fig. 6 was calculated with parameter values obtained in this experiment. Because in this experiment conductance was measured only in the presence of toxin, a_g and V_g were taken to be equal to a_g^* and V_g^*, respectively. It could not essentially affect the result of the calculations, since parameters of the conductance change only slightly after toxin treatment (see Table I). For calculating the K_A-curve in Fig. 7, mean parameter values obtained from nine experiments were used. The agreement between calculation and experiment is rather good.

Preliminary structural studies show that molecules of the toxin possess a hydrophobic part, or 'leg'. One may imagine that this 'leg' being plunged into the lipid matrix of the membrane imposes a restriction on inactivating displacement of charged particle(s) or dipole(s) in the channel. A lesser distance travelled by this charged particle(s) in an electric field in the poisoned channel as compared with the normal one accounts for a lower value of the effective charge of the inactivation transition and a lower slope of the h_∞-curve, respectively.

As noted above, K_A has a relevance only to channels which are not inactivated by the slow mechanism. The model similar to that given above, but more general, gives the following equation for the overall binding constant (K_Σ):

$$K_\Sigma = \frac{S_\infty}{S_\infty^*} \cdot \frac{h_\infty}{h_\infty^*} \cdot \frac{1 + \exp a_2^*(V_M - V_2^*)}{1 + \exp a_2(V_M - V_2)} = K_A \cdot \frac{S_\infty}{S_\infty^*} \tag{16}$$

Since $S_\infty^* \geqslant S_\infty$ (see Figs. 3 and 7), $K_\Sigma \leqslant K_A$. This means that the channels inactivated by the slow mechanism have a lower binding constant than non-inactivated channels. Substitution of the mean values of the parameters a_s, a_s^*, V_s and V_s^* into Eqn. 16 shows that K_Σ decreases by a factor of about 60 as the potential is shifted from −80 to 0 mV.

K_Σ, by virtue of its significance, is quite analogous to the binding constant determined via direct measurement of an amount of labelled toxin [7]. According to the above consideration, the decrease of the toxin binding upon depolarization is due largely to a transition of the sodium channels to a state of fast inactivation and dependence of the binding constant of inactivated channels on potential as such. To a rather lesser degree, it is due to the transition of the channels into a state of slow inactivation.

References

1 Koppenhöfer, E. and Schmidt, H. (1968) Pfluegers Arch. 303, 133—149

2 Narahashi, T., Shapiro, B.J., Deguchi, T., Scuka, M. and Wang, C.M. (1972) Am. J. Physiol. 222, 850—857

3 Romey, G., Chicheportiche, R., Lazdunski, M., Rochat, H., Miranda, F. and Lissitzky, S. (1975) Biochem. Biophys. Res. Commun. 64, 115—121

4 Bernard, P., Courad, F. and Lissitzky, S. (1977) Biochem. Biophys. Res. Commun. 77, 782—788

5 Okamoto, H., Takahashi, K. and Yamashita, N. (1977) Nature 266, 464—467
6 Catteral, W.A., Ray, R. and Morrow, C.S. (1976) Proc. Natl. Acad. Sci. U.S.A. 73, 2682—2686
7 Catteral, W.A. (1977) J. Biol. Chem. 23, 8660—8668
8 Mozhayeva, G.N., Naumov, A.P., Grishin, E.V. and Soldatov, N.M. (1979) Biofizika, 24, 235—241
9 Grishin, E.V., Soldatov, N.M., Tashmuchamedov, B.A. and Atakusiev, B.U. (1978) Bioorg. Chim. 4 450—461
10 Mozhayeva, G.N., Naumov, A.P., Negulyaev, Yu.A. and Nosyreva, E.D. (1977) Biochim. Biophys Acta 466, 461—473
11 Koppenhöfer, E. (1967) Pfluegers Arch. 293, 34—55
12 Koppenhöfer, E. and Vogel, W. (1969) Pfluegers Arch. 313, 361—380
13 Hille, B. (1967) J. Gen. Physiol. 50, 1287—1302
14 Hodgkin, A.L., Huxley, A.F. and Katz, B. (1952) J. Physiol. 116, 424—448
15 Taylor, R.E., Moore, J.W. and Cole, K.S. (1960) Biophys. J. 1, 161—202
16 Drouin, H. and Neumke, B. (1974) Pfluegers Arch. 351, 207—229
17 Oxford, G.S. and Pooler, J.P. (1975) J. Gen. Physiol. 66, 765—779
18 Chandler, W.K. and Meves, H. (1970) J. Physiol. 211, 707—728
19 Fox, J.M. (1976) Biochim. Biophys. Acta 426, 232—244
20 Schauf, C.L., Pencek, T.L. and Davis, F.A. (1976) Biophys. J. 16, 771—777
21 Brismar, T. (1977) J. Physiol. 240, 283—297
22 Rudy, B. (1978) J. Physiol. 283, 1—22
23 Bergman, C., Dubois, J.M., Rojas, E. and Rathmayer, W. (1976) Biochim. Biophys. Acta 455, 173-184
24 Chiu, S.Y. (1977) J. Physiol. 273, 573—596
25 Hille, B. (1978) Biophys. J. 22, 283—294
26 Hodgkin, A.L. and Huxley, A.F. (1952) J. Physiol. 116, 500—544
27 Bezanilla, F. and Armstrong, C.M. (1977) J. Gen. Physiol. 70, 549—566
28 Armstrong, C.M., Bezanilla, F. and Rojas, E. (1973) J. Gen. Physiol. 62, 375—391
29 Hill, T. and Chen, Y.D. (1972) Proc. Natl. Acad. Sci. U.S.A. 69, 1723—1726
30 Stevens, C.F. (1978) Biophys. J. 22, 295—306
31 Chandler, W.K. and Meves, H. (1970) J. Physiol. 211, 653—678